Title: Sustainable membrane-coated electrodes for CO2 electroreduction to methanol in alkaline media

Autores: Aitor Marcos-Madrazo, Dr. Clara Casado-Coterillo, Prof. Angel Irabien

Revista: ChemElectroChem
Editorial: Wiley-VCH
Factor de impacto 2018: 3,975 (5-year IF of 4.200)
Fecha de aceptación: 8/10/2019
Fecha de publicación online: 8/10/2019
DOI: http://dx.doi.org/10.1002/celc.201901535.

Sustainable membrane-coated electrodes for CO_2 electroreduction to methanol in alkaline media

*Aitor Marcos-Madrazo, Dr. Clara Casado-Coterillo *, Prof. Ángel Irabien.*

Department of Chemical and Biomolecular Engineering, Universidad de Cantabria, Av. Los Castros s/n, 39005 Santander, Spain

*Corresponding author: Clara Casado-Coterillo, e-mail: casadoc@unican.es; tel: +.34 942206777

ABSTRACT

CO_2 electroreduction has high potential to combine Carbon Capture Utilization and energy storage from renewable sources. The key challenge is the construction of highly efficient electrodes giving optimal CO_2 conversion to high-value products. In this regard, research on electrode structures remains as an important task to face. Despite the advancements in gas diffusion electrodes (GDEs) to facilitate CO_2 transfer and electrode efficiency, catalyst is still vulnerable to be swept by the gas and the liquid electrolyte, reducing the stability. We report the fabrication of novel membrane coated electrodes (MCEs), by coating an anion exchange membrane over a copper (Cu):chitosan (CS) catalyst layer onto the carbon paper. CS and poly(vinyl) alcohol (PVA) were chosen for membrane preparation and catalyst binder, where Cu was embedded in the polymer matrix as nanoparticles or ion-exchanged in a layered stannosilicate or zeolite Y, to improve their hydrophilic, conductive, mechanical and environmentally-friendly properties considered relevant to the sustainability of the electrode fabrication and performance. The intimate connection between the CS:PVA polymer membrane over-layer and the CS/Cu catalytic layer

protects the MCEs from material losses, enhancing the CO_2 conversion to methanol, even in high alkaline medium. A maximum Faraday Efficiency to methanol of 68.05% was achieved for the 10CuY/CS:PVA membrane over-layer.

INTRODUCTION

Over the past few years, we have observed how the impacts of climate change throughout the planet are increasing dramatically, and so is the global urgency to take measures against them. As a matter of fact, two different observatories have recently recorded the alarming concentration of carbon dioxide in the atmosphere of 415 ppm [1,2]. Therefore, different techniques for the Carbon Capture, Utilization and Storage (CCUS) are being studied to reduce CO_2 emissions and to use it as raw material in industry, in response to the Circular Economy [3]. The combination of CCUS with a renewable energy production model makes the electrochemical reduction of CO_2 (CO_2RR) a plausible technological alternative, by simultaneously confronting the energy storage from renewable sources and the CO_2 transformation into value added products [4].

However, the electrochemical conversion of CO_2 is still a challenging subject. One of the main issues is the fabrication of electrodes that provide productive and efficient transformation of CO_2 at low overpotentials. To this effect, it is important to improve the effectiveness and selectivity of complex electrocatalysts [5]. Electrocatalysis is an interfacial phenomenon, where the relative ratio of CO_2 and H_2 (H^+) is dictated by the intrinsic selectivity of surface active sites and the local concentration of reaction compounds involved in the different rate-controlling stages. Therefore, there is an urgent need for understanding the mechanisms involved in order to design more effective electrodes [6,7]. In this regard, many researchers focus on the catalyst composition, being copper one of the most studied metals [8–11]. Besides composition, surface structure and

morphology also plays a relevant role in electrode performance. The effect of surface morphology on the CO_2RR to alcohols or hydrocarbons has been studied in the form of Cu-coated nanospikes [12], nanowires [13] or Metal Organic Frameworks (MOFs) [14,15], among others. The micro and meso structure of the electrode determines the diffusional gradients under steady-state conditions. Steady-state conditions are the most commonly investigated in CO_2/HCO_3^- electrolytes because their slow equilibration kinetics leads to the mass transfer limited region. In order to facilitate CO_2 transfer to the catalyst and improve the performance of the electroreduction process, researchers have applied high pressure [16], gas diffusion electrodes (GDEs) [17,18], taking advantage of the higher surface of catalyst accessible to the CO_2, and metal coated ion-exchange membrane electrodes (CCMs) [19]. However, material losses and degradation hinder the durability of the electrodes in continuous flow electrochemical cells for CO_2 reduction [7,19,20].

Apart from the electrodes and catalysts, another important device that may play a significant role in the electrolytic cell are the *ion exchange membrane* (IEM) [21,22] and the electrochemical environment [5]. The most studied configuration in flow reactors are membrane reactors, where the membrane role consists just on the physical barrier that separates the anode and the cathode and facilitates the selective transport of ions between them to close the circuit, while simultaneously attenuating the cross-over in the opposite direction and the re-oxidation of the product.[23] In order to avoid the challenges of using liquid electrolytes, to improve CO_2 solubility and recovery of liquid products, solid polymer electrolyte membranes were introduced in the design of electrochemical flow reactors [7,19,20]. The development of alkaline anion–exchange membranes (AAEMs), bipolar membranes and mosaic membranes in opposition to most conventionally employed cation exchange membranes (CEMs), Nafion 117 (DuPont) [24–26], is an example of the increasing relevance that the role of the IEM in the electrochemical reaction is

gaining in research literature [10]. Despite the predominance of CEMs, the most widely studied electrochemical environment for CO_2RR is slightly alkaline (almost neutral) rather than acid medium, in order to reduce the influence of the Hydrogen Evolution Reaction (HER) that otherwise competes with CO_2RR. Thus, AAEMs are attiring the attention as to their suitability for this process [4,27]. Also, high alkaline pH has been observed to influence CO_2 reduction on Cu catalyst surfaces, due to the hydroxide ions role in modulating the catalyst surface and suppressing the HER [19]. AAEMs work by facilitating the flow of anions (e.g. OH^-) from the cathode to the anode. In CO_2 electrolyzers working in alkaline conditions, OH^- ions rapidly react in the presence of CO_2 to form HCO_3^- and CO_3^{2-} but the lower mobility of the latter ions compared to OH^- usually inhibit ion transport and reduce CO_2 reduction efficiency [19]. Thus the anion transport mechanism is expected to be more limiting for CO_2RR with systems using AAEMs than CEMs because the forward reaction of CO_2 to products is encouraged without delivering H^+ to the cathode. And yet, some of the best performing CO_2 flow cells known today use AAEMs [28,29]. Through commercial anionic membranes as FAA-3 (Fumatech) [30] or A-901 (Tokuyama) [31], the rate of product cross-over was proportional to the current density. Aeshala et al. highlighted the improved CO_2RR efficiency of quaternary ammonium groups in anionic solid polymer electrolytes.[32] Dioxide Materials developed Sustainion@, an AAEM containing imidazolium compounds that improve the performance and selectivity of CO_2RR to CO [28,29,33]. However, these membrane materials and preparation are usually expensive or highly toxic to health and environment. Thereby, the search for renewable and more economic polymers in membrane preparation is a key factor to ensure the future sustainability of the process [34]. There, chitosan (CS) is a great alternative in this regard and its use in electrochemical devices has been reviewed [35], leading to intensive work, especially in the framework of alkaline fuel cells [36]. The conductivity and the mechanical stability of CS can

be tuned up by blending with low-cost poly(vinyl alcohol) (PVA), and different metal or ion-exchange porous structured fillers embedded in the polymer matrix, for further functionalizing the membrane properties for electrochemical applications, by the Mixed Matrix Membranes (MMM) approach [37].

Then, the concept of membrane coated electrocatalysts (MCEC) came across recent literature, as an alternative to improve the stability of electrocatalysts for electrochemical devices, from sensors to fuel cells, as a mean of controlling the interfacial phenomenon of electrocatalysis and the local concentration of reaction compounds and catalyst sites involved in the different rate-controlling stages [38]. Likewise, the encapsulation of metal electrocatalysts in different matrices has been reported to have a significant influence on the CO_2RR selectivity and stability, depending on the nature of the polymer. Protective membrane layers composed of metal oxides [39,40] have been proposed for HER and Methanol Oxidation Reaction, and conductive polymers [41–45] have been studied for the CO_2 electroreduction at chemistry laboratories, where the polymer both protects the catalytic layer and boosts the ion transport to the active sites, thus reducing the required over potentials [42,46] and slightly improving the efficiency of the CO_2 electrochemical reduction in different media. This creates a new field for research that we may call “membrane coated electrodes (MCEs)”. As an example, polypyrrole (Ppy) coating has been recently observed to increase the stability, conductivity, and catalytic activity of Cu_2O shape structures on paper electrodes in CO_2RR in aqueous electrolyte medium [47]. With these new MCE structures, new reaction pathways and mechanisms may be possible, and the product selectivity can be tuned up by applying a transport-mediated reaction selectivity and the protective layers controlling the mass and ion transport to the metal electrocatalyst, by anticipating that rapid transport to the electrode and through a thin membrane and analyte pre-concentration in the membrane improve the

sensitivity of the system [38]. Likewise, we believe that the dispersion of metal particles into a conductive polymeric matrix may provide synergies with the specific areas of metal catalyst and thus improve the catalytic efficiency [37]. For instance, the hydrophilicity and crossover, a major challenge in fuel cells, has been controlled by coating a silica sol-gel derived over-layer to Nafion membranes [40].

The improvement on anion conductivity, mechanical resistance and hydrophilic character is desirable for an overall better behavior of the MCE. In this work, GDEs for the electroreduction of CO_2 have been prepared using Cu nanoparticles (NPs) and CS biopolymer solution as binder of the catalytic layer sprayed on carbon paper, instead of Nafion (DuPont) or Fumion (Fumatech). The MCE was prepared by coating a membrane over-layer on top of the new GDE. This membrane over-layer was composed of a CS:PVA equimolar blend filled by different Cu-containing inorganic fillers, whose effect on the physico chemical and mechanical properties, among other features, was correlated with the membrane composition in a previous work [48]. The aim of the present work is evaluating whether the controlled anion conductivity, mechanical resistance and hydrophilic character of this membrane layer provides catalytic to the MCE in the CO_2RR to other products, and simultaneously provides surface electrode protection in terms of electrode efficiency and stability in an undivided electrochemical cell. As such, the alkaline anion exchange membranes (AAEMs) composed of Cu/CS:PVA, Cu-UZAR-S3/CS:PVA and Cu-Y/CS:PVA mixed matrix membranes (MMMs) were selected as membrane over-layer in this work on account of the permeability, hydrophilicity and conductive and mechanical resistance, respectively. A pure CS:PVA polymer membrane over-layer was also characterized in this work, as well as an uncoated GDE without membrane over-layer were also evaluated for comparison purposes.

EXPERIMENTAL METHODS

Preparation of CS:PVA polymer coated electrodes

The prepared MCEs were composed of three layers, as schematized in the configuration plotted in Figure 1, consisting of a bottom porous carbon paper (Toray TGP-H-60) acting as conductive macroporous support and gas diffusion layer (GDL), a catalytic layer where the catalytic ink is composed of Cu NPs (60-80 nm Sigma Aldrich, Spain) and CS aqueous solution, prepared from a 1 wt. % solution of CS (coarse ground flakes and powder, 310,000 - 375,000 Da and 75% deacetylation degree, Sigma Aldrich) as binder, and a membrane over-layer over the GDE. The catalyst:binder mass ratio was 70:30 in all cases. Water was added to the binder as vehicle and the final concentration of solids (Cu + CS) was 3 wt. %. The ink was sonicated for 20 min and air-brushed onto the carbon paper. For the membrane over-layer fabrication, an equimolar blend of CS and PVA (powder, 85,000 - 120,000 Da and 99+% hydrolyzed, Sigma Aldrich) were stirred for 24h, from previously prepared aqueous solutions of CS 1 wt. % and PVA 4 wt. %, respectively.[48] The polymer solution was cast over the GDE (carbon paper + catalytic layer) and left drying overnight at room temperature. When the solvent was evaporated, the solid membrane layer was perfectly fixed and integrated as part of the electrode. Electrodes were then immersed in NaOH 1M for the activation of the alkaline anion exchange membrane (AAEM) over-layer. The geometric surface area of the electrodes was 10 cm^2 and its catalytic loading, 1 mg/cm^2.

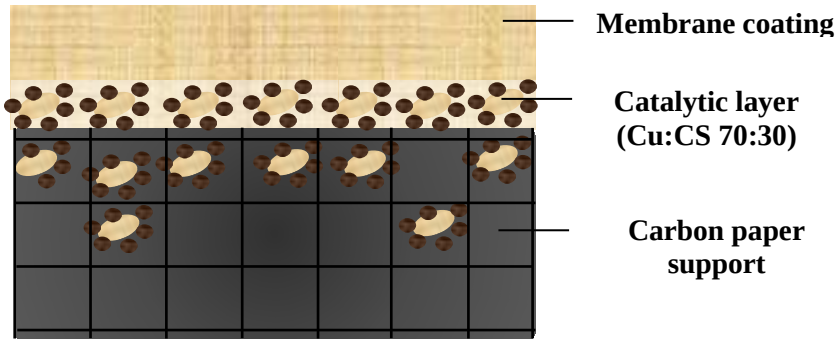

Figure 1. Schematic representation of the MCE (Membrane-coated electrode) configuration proposed in this study.

Preparation of mixed matrix membrane coated electrodes

The same procedure was followed for the preparation of the mixed matrix MCEs, by adding different Cu-based fillers to the polymeric CS:PVA blend prior to the casting over the catalytic layer. Three fillers were selected from our previous work, on account of their water uptake and water vapor permeability, ion exchange capacity and conductivity, and tensile strength, respectively: commercial Cu NPs, Cu-exchanged on layered stannosilicate UZAR-S3 (Cu-UZAR-S3) or zeolite Y (Cu-Y).[48] It was expected that the implications observed on the stability of the Cu oxidation state in Cu NPs, Cu-exchanged in layered silicates and Cu-exchanged in zeolites may lead to a different catalytic activity of the MCE, and not only due the Cu additional content. Cu-UZAR-S3 and Cu-Y selected loadings were 10 wt. % of the total solid content of the membrane, as the optimal from the previous work,[48] while for Cu NPs, the filler loading was kept below 5 wt.% because the addition of higher Cu NPs loadings decreased the solution viscosity so much that the membrane casting upon MCE preparation was very cumbersome. Table 1 enumerates the different electrodes prepared as a function of membrane over-layer composition.

Table 1. List of electrodes prepared as a function of membrane coating layer composition.

Electrode description	**Support (200 µm)**	**Catalytic layer (1 mg Cu/cm^2)**	**Membrane coating composition**	**Thickness of the membrane layer, *b* (µm)**
No coating	Carbon paper	Cu NPs	-	-
CS:PVA	Carbon paper	Cu NPs	CS:PVA	51 ± 1.71
Cu-UZAR-S3/CS:PVA	Carbon paper	Cu NPs	10Cu-UZAR-S3/CS:PVA	46 ± 1.63
Cu-Y/CS:PVA	Carbon paper	Cu NPs	10Cu-Y/CS:PVA	47 ± 3.77
Cu/CS:PVA	Carbon paper	Cu NPs	5Cu/CS:PVA	44 ± 1.83

Characterization

The surface morphology and Cu dispersion of the electrodes was carried out by scanning electron microscopy on a FEI Inspect F50 microscope at the Universidad de Zaragoza (Spain). The thicknesses of all the layers of the MCE were measured at several spots over the surface area of each electrode using an IP-65 Mitutoyo digital micrometer (Japan).

Electrochemical experiments

The electrochemical behavior was first studied by performing cyclic voltammetry (CV) on the as-prepared electrodes in Table 1, using a potentiostat (MSTAT4, Arbin Instruments) at a scan rate of 0.1V/s between 0 and -2V vs Ag/AgCl until reproducible voltammograms were obtained. An open undivided three electrode cell was employed. Each electrode prepared in this work (Table

1) was tested as working cathode, while glassy carbon was used as counter electrode and Ag/AgCl (KCl saturated) as the reference electrode. An aqueous solution of KOH 1M was prepared as the electrolyte, bubbled for 30 min with either CO_2 or N_2 prior to the CO_2 saturated and deareated experiments, respectively. Current densities (*j*) were calculated by normalizing the current generated with the surface area of the cathode.

Experiments at fixed constant potentials were carried out on fresh electrode samples using the same electrochemical cell. The same solution of KOH was employed as electrolyte, saturated with CO_2 before the experiments and continuously aerated during the electro reduction process. Potentials over Ag/AgCl were set at -0.3V, -0.5V, -1.0V and -1.5V, after the CV observations. The duration of each experiment was 60 min. To determine product composition and concentration, liquid samples were taken and analyzed via gas chromatography-mass spectrometry (GC-MS-QP2010 Ultra, Shimadzu). The efficiency of the electron transfer towards the reduction of CO_2 to products was determined by calculating the Faraday Efficiency (FE) to main products detected for every experiment, using Equation (1).

$$\mathrm{FE}(\%) = \frac{\mathrm{znF}}{\mathrm{q}} \qquad (1)$$

where *z* is the number of electrons exchanged, n is the moles of product generated, *F* is the Faraday constant (96484.5 C/mol) and *q* is the total charge applied, in Coulombs.

Results

Electrochemical characterization

Figure 2 plots the CV diagrams obtained. The voltammogram of a Cu plate was included for comparison in Figure 2a. The pH of the KOH 1M electrolyte solution was 14.07 as-prepared and after aeration with N_2, while this value descended to 10.5 after saturation with CO_2 due to

partial carbonation of KOH, which was constant along the voltammetry electrolysis experiment as was the pH. The potential was referred to the Reversible Hydrogen Electrode (RHE) as $E_{vs\ RHE} = E_{vs\ Ag/AgCl} + 0.197 + 0.059 \cdot pH_{electrolyte}$, where $pH_{electrolyte}$ was the initial pH of the solution [49], in order to compare with literature.

In Figure 2, the reduction activity observed in the red voltammograms (no CO_2) can be only be attributed to the electrode or H_2O reduction (HER) contributions. Aydin et al. reported that at -0.7V vs Ag/AgCl, Cu wire presented a reduction peak [42] as the one appreciated for the Cu plate (Figure 2a) and the uncoated GDE (Figure 2b) in this work at lower overpotentials. A large oxidation activity was appreciated in the reverse scan, most remarkable in the Cu plate, which implies that the continuous metal plate electrode was extremely vulnerable to redox reactions during CV [49]. This oxidation activity was also observed, though less pronounced, in the uncoated CS:PVA/Cu GDE. This may be attributed to the structural differences between the Cu continuous plate and the Cu:CS GDE, although it has been hypothesized that the binding of an ionic polymer, *i.e.* CS, with the metal ion may slightly protect the Cu NP catalyst in the catalytic layer (Figure 1)[50] from degradation, which does not occur in the Cu plate. This protection may also slightly reduce the number of active sites available for the reaction, while enhancing the activity of those that are indeed available, compared with the metal plate. In this sense, the MCEs seemed passivated since their voltammograms in Figures 2c-2f do not show those electrode contributions, so it can be expected that the membrane over-layer successfully reduced the degradation of the catalytic layer.[43] For all the electrodes tested, notorious current reductions were observed at overpotentials higher than -0.5V vs RHE, where HER is the predominant reaction.[17,51]

In the CO_2 saturated electrolyte, a reduction peak appeared at 0.25V vs RHE, attributed to CO_2RR. This reduction activity was more significant for the MCEs with Cu-UZAR-S3/CS:PVA

and Cu-Y/CS:PVA MMMs as membrane over-layers, whose voltammograms are represented in Figures 2e and 2f, respectively. Therefore, it could be advanced that the enhanced hydrophilicity, ion exchange capacity and anion conductivity of these membranes observed in our previous work,[48] may be leading to an improvement of the electrode behavior in CO_2 electrochemical reduction.

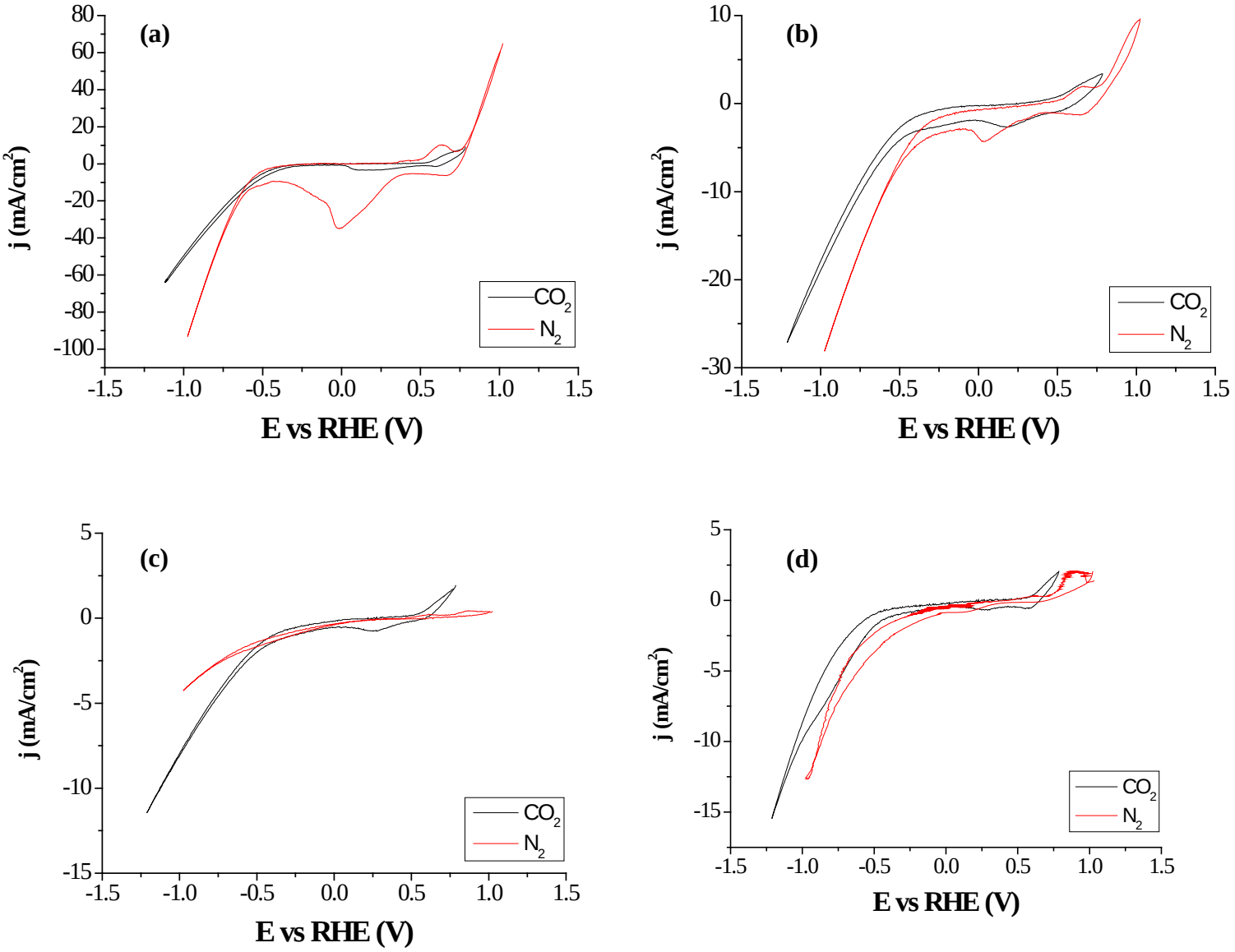

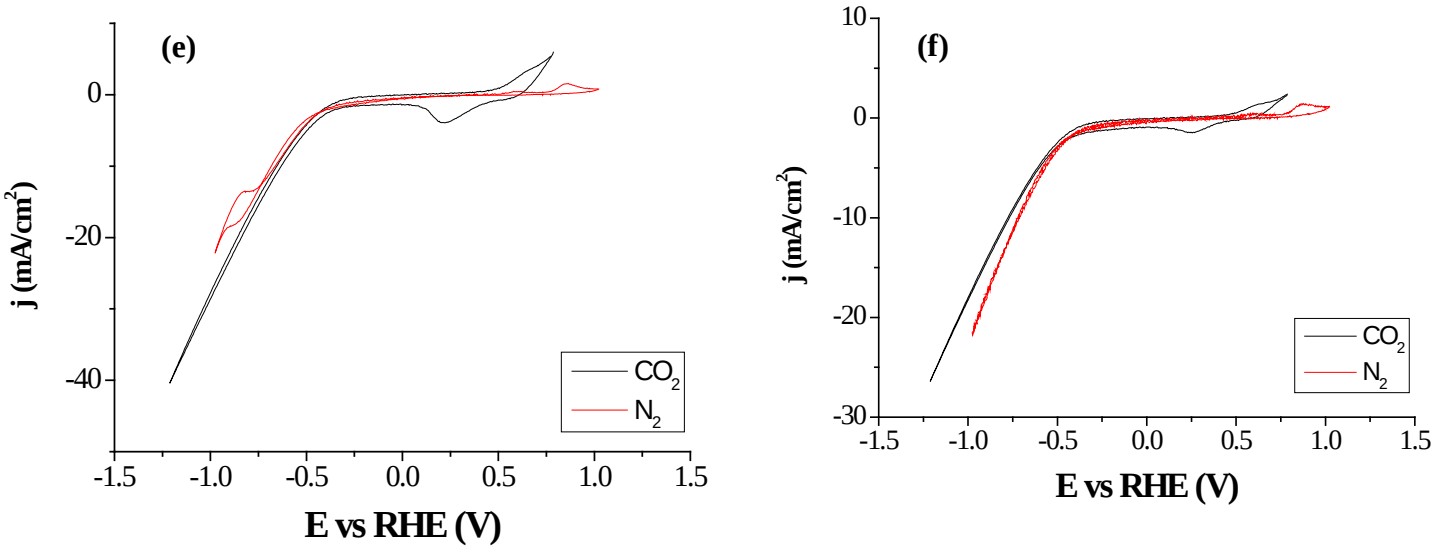

Figure 2. Cyclic Voltammetry curves obtained in the electrochemical study in the presence and absence of CO_2 for (a) Cu plate, (b) uncoated GDE, (c) CS:PVA polymer MCE, (d) Cu/CS:PVA MCE, (e) Cu-UZAR-S3/CS:PVA MCE, and (f) Cu-Y/CS:PVA MCE.

Electrochemical reduction of CO_2

Electroreduction experiments at constant potentials of -0.3V, -0.5V, -1.0V and -1.5V vs Ag/AgCl were carried out for 1h. These potential values were selected in agreement with the different stages observed in the CVs in Figure 2: at -0.3V, a first reduction process was observed, at -0.5V, we identified the CO_2RR reduction process, at -1.0V, another reduction began, generating a high current density and, finally, at -1.5V, a great reduction current was involved, primary attributed to HER.

The current density generated at these potentials was stable over the full length of the experiments, as represented in Figure 3a, so steady state conditions were confirmed. Faraday

Efficiencies (FE) for methanol production along the experiment time are also represented in Figure 3b, observing that they did not suffer from large variations either.

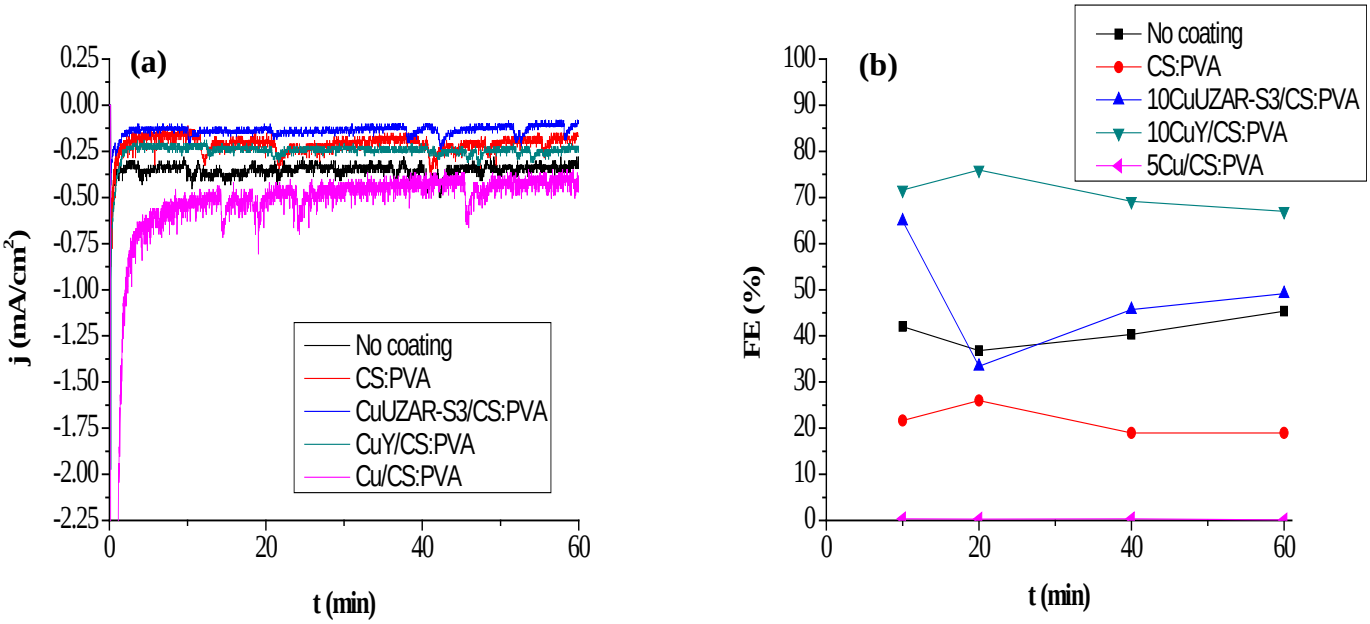

Figure 3. a) Chronoamperommetry carried out at -1.0 V for the prepared electrodes and b) FE for methanol at -1.0V at the times when the samples were taken.

Table 2 presents the main results obtained in the CO_2 electroreduction experiments at -1.0V and -1.5V vs Ag/AgCl (-0.18V and -0.68V vs RHE, respectively) for the electrodes prepared in this work. Both the uncoated Cu/CS GDE and the MCEs led to methanol as main product, which is attributed to the alkaline environment,[5] as well as water swelling[11,48] and surface morphology.[12] Some Cu-based GDEs from literature also directed to methanol as main product are also reviewed in Table 2 in order to verify that the current densities generated with our working

electrodes were of the same order of magnitude as those reported by other researchers in undivided cells at low overpotentials.[52] For all the electrodes tested in this work, the current densities increased with increasing potential, although the lower potentials (-0.5V and -0.3V vs Ag/AgCl) are not included in Table 2 because the current densities generated in those conditions were too low to make the calculations reliable. The decreasing FE to methanol with increasing potential and current density at higher over-potentials can be allocated to the HER as the dominating reaction [17,51]. The uncoated GDE prepared in this work generated higher current densities and increased methanol production than the pure CS:PVA MCE, with a FE for methanol of 40.11% and 19.71%, respectively. These results are attributed to the higher accessibility of CO_2 to the catalyst in the uncoated GDE, and confirmed that the membrane over-layer was posing an additional resistance to transport. This additional step was also observed for the Cu/CS:PVA MCE, with a lower activity than the pure CS:PVA polymer MCE, but it was not observed for the Cu-UZAR-S3/CS:PVA or Cu-Y/CS:PVA MCE. This could be related to the differences in water uptake, water permeability and anion conductivity among the Cu-UZAR-S3/CS:PVA, Cu-Y/CS:PVA and Cu/CS:PVA MMM over-layers observed previously.[48]

Table 2. The current density and corresponding FE(CH_3OH) under controlled potential electrolysis at -1.0V and -1.5V vs. Ag/AgCl (-0.18V and -0.68V vs RHE) in different electrodes to methanol.

Electrode	**Electrolyte media**	**E vs RHE (V)**	j_{geom} **(mA/cm^2)**	**FE (CH_3OH) (%)**
Ru-based CCM [53]	Gas phase	0.46	0.90	0.93

Electrode	Electrolyte media	E vs RHE (V)	j_{geom} (mA/cm^2)	FE (CH_3OH) (%)
Cu-TiO_2/NG based GDE [54]	Near neutral (pH=6.8)	-0.20	-0.06	19.5
Cu-doped CNTs based GDE [55]	Alkaline (pH=9)	0.28	-4.75	47.4
Cu-Bi MOFs based GDE [15]	Near neutral (pH=6.8)	0.21	-10.0	18.2
Cu_2O(ML-OH)/Ppy on paper	Neutral (pH = 7.6)	0.85	0.22	93
Cu/CS:PVA GDE [This work]	Alkaline (pH=10)	0.18 0.68	0.35 3.35	40.1 1.74
CS:PVA MCE [This work]	Alkaline (pH=10)	0.18 0.68	0.21 1.13	19.7 2.06
Cu-UZAR-S3/CS:PVA MCE [This work]	Alkaline (pH=10)	0.18 -0.68	0.14 1.59	41.6 2.22
Cu-Y/CS:PVA MCE [This work]	Alkaline (pH=10)	-0.18 -068	0.25 4.86	68.0 0.27
Cu/CS:PVA MCE [This work]	Alkaline (pH=10)	-0.18 -0.68	0.59 7.28	2.98 0.15

After the experiments with the uncoated Cu-CS:PVA GDE, material losses were visually noticed that were not observed after the experiments conducted with the MCEs. The Cu content of the electrodes of the uncoated GDE was 4.38 ± 2 wt. %, 18 ± 7 wt. % for the CS:PVA (Figure 4b) and 21.43 ± 1.6 wt. % for the Cu/CS:PVA (Figure 4c) MCEs. The Cu content decreased for the MCE where the membrane over-layer was composed of the Cu-Y/CS:PVA MMM materials to a value of 13 ± 4 wt. % (Figure 4d). The particular performance of the Cu/CS:PVA MCE could be a consequence of the low viscosity of the Cu CS:PVA polymeric blend solution causing densification of the membrane over-layer upon casting and solvent evaporation, as well as the largest water transport reported elsewhere [48]. Therefore, this Cu/CS:PVA membrane layer generated the highest current densities generated of all MCE in Table 2, but the catalyst in metallic form seemed to be less accessible for CO_2 and its ionic forms, so the methanol production dropped, in favor of HER as dominant reaction.[56]

As Cu in other polymer-coated electrodes studied in the state of Cu(II) [48], their efficiency towards CO_2 conversion was enhanced by the polymer coating. Aydin et al. observed that coating Cu-derived NPs with conductive polypyrrole over a Nafion 117 membrane, controlled the HER, compared to blank Cu as electrocatalyst, with a FE of 25% and 20% towards CH_4 and formate, respectively, thus shifting the product selectivity and catalyst activity.[42] Grace et al. observed an improvement in the FE of CO_2 to acetic and formic acids by coating Cu_2O NPs electrodes with a polyaniline film,[57] even at low overpotentials. Ahn et al. reported that the coating of Cu foam electrode surfaces could both activate and stabilize the electrode surface towards different reaction intermediates.[58] Conductive polypyrrole could also increase the stability of Cu_2O NPs in the CO_2RR to methanol [47].

The diffusion layer thickness can be estimated using the Nernst diffusion layer Equation (2),

$$I_{ss} = \frac{nFADC^*}{\delta} \quad (2)$$

where I_{ss} is the steady state current, D is the diffusion coefficient of CO_2 (1.9 x 10^{-5} cm^2/s at room temperature [59]), C is the dissolved CO_2 (aq) concentration in a fully saturated solution, 0.034 M [60]), A, the geometric area of the working electrode and δ (cm) the diffusion layer thickness. The value obtained for the uncoated Cu:CS GDE in this work was of the same order of magnitude obtained in literature with other GDEs, so Equation (3), modified for a planar electrode by Billy and Co,[59] could be applied to calculate the diffusion layer thickness of our MCE, as

$$\delta = 0.68D^{1/3}\left(\frac{1}{b}\right)^{2/3}A^{1/3}v^{-1/3} \quad (3)$$

where v is the estimated average CO_2 flow rate, which in this work is 1 mL/min, and b as the membrane over-layer thickness in Table 1. The values obtained for δ were 196 cm, 264 cm, 241 cm and 230 cm, for the CS:PVA, Cu/CS:PVA, Cu-UZAR-S3/CS:PVA and Cu-Y/CS:PVA MCE, respectively. These values are higher than those reported in literature,[58,59] though, confirming the additional resistance opposed by the membrane over-layer and expecting the existence of non-idealities when this membrane over-layer is a mixed matrix membrane (MMM),[61,62] but yet the diffusion layer values correlated with the SEM observations taken of the surface morphologies of the electrodes after the electroreduction experiments, discussed below regarding Figure 4.

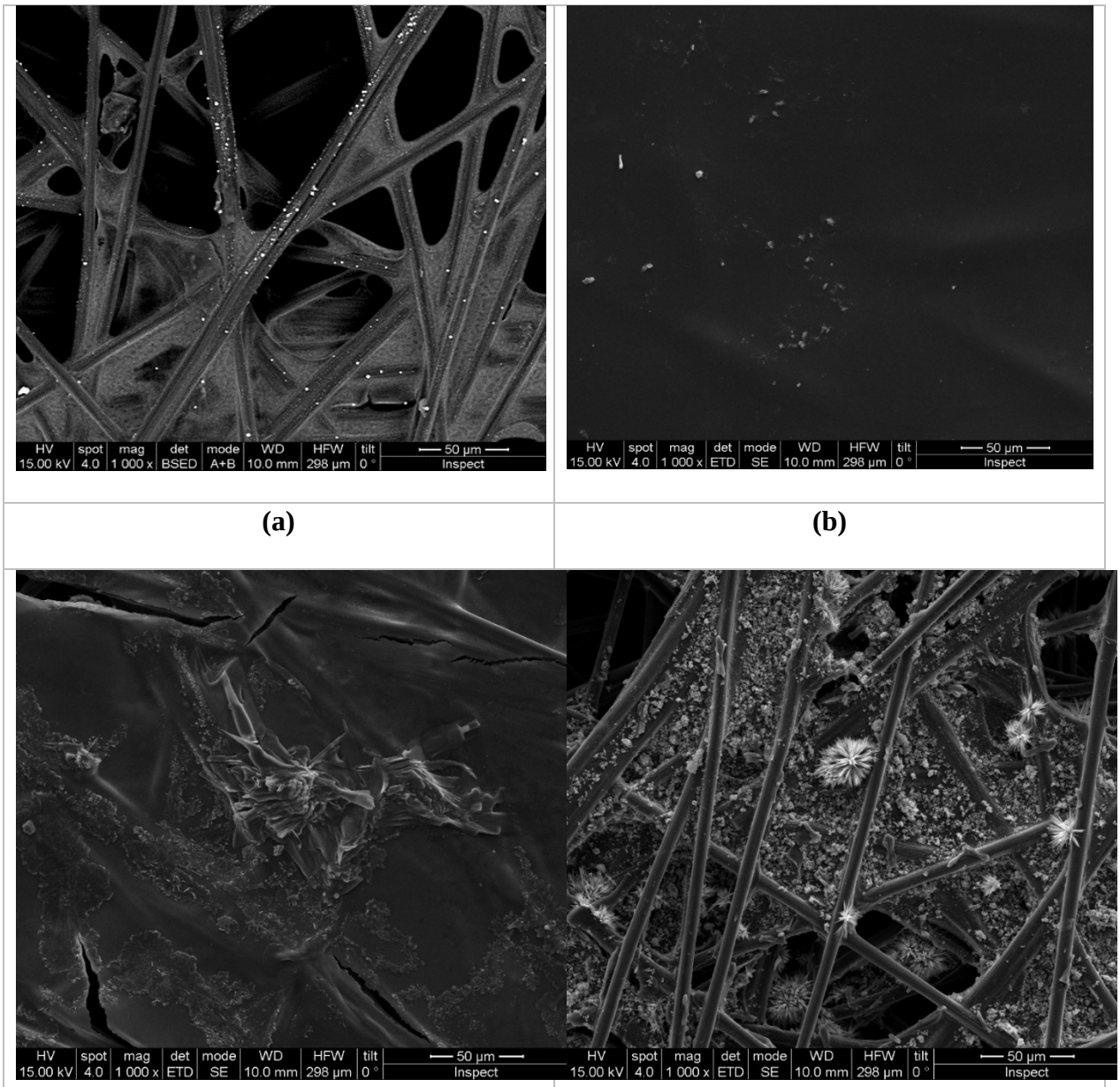

Figure 4. SEM images of the MCE prepared in this work: (a) uncoated GDE, (b) CS:PVA MCE, (c) Cu/CS:PVA MCE and (d) Cu-Y/CS:PVA MCE. Magnification is 50 µm.

Because the CS:PVA MCE showed a better performance than the uncoated GDE prepared in this work, this was first attributed to the protection provided by the membrane over-layer and

the CS binding properties in the catalytic layer mentioned earlier.[58] The encapsulation of a nanoparticulate metal catalyst in a membrane over-layer with OH^- functional groups that interact with the catalyst active sites and CO_2-derived reagents can avoid the dissolution of metal NPs and facilitate the membrane fabrication in a mixed matrix containing ions.[38] The membrane over-layer of the Cu/CS:PVA MCE (Figure 4c) was thinner than that of the CS:PVA MCE (Figure 4b) after the electrolysis experiments. When the CS:PVA matrix of the membrane over-layer contained Cu exchanged in inorganic zeo-type fillers, although the oxidation state, hydrophilic, transport and mechanical properties were more promising than the pure CS:PVA polymer membrane material, as analyzed elsewhere,[48] Figure 4d reveals that this layer has collapsed into the carbonaceous porous support below, probably due to local decreases of pH in the electrode surface along the experimental run. The CS tends to dissolve in weak acid solutions and the longer stability of the Cu ion active for CO_2RR when exchanged in zeolites and layered silicates as compared to the free metal NPs observed in our previous work may be lowering the local pH of the MCE surface.[63] Nevertheless, the EDX analysis revealed that both the Cu catalyst from the membrane over-layer and the NPs from the intermediate catalyst layer were present in the pores of the Toray paper, attaining a remarkable FE to methanol of 68.05% in the case of the Cu-Y/CS:PVA MCE at an over-potential of -0.18V vs RHE, as was already shown in Table 2. The design and tuning of the MCEs using renewable or low-cost polymer materials for the membrane over-layer and the binder of the catalytic layer can therefore be an attractive strategy toward enhancing the CO_2RR performance in membrane-like reactors needed for large-scale implementation.[64]

Commentaries on the hypothesized CO_2 reduction mechanism

The half-reactions we believe that are taking place in the anode and cathode, from analyzing the scarce, but growing, literature on CO_2 reduction in alkaline media, will be presented here in an attempt to start explaining the experimental results described above. The electrolyte in this work was KOH 1M or 2M (no differences in CV performance were observed in the laboratory upon increasing the electrolyte concentration, so we focused to 1M), and taking into account that the solubility of CO_2 in water 0.036M at STP conditions,

$$CO_2\ (g) \rightarrow CO_2(aq) \quad (4)$$

The dissolution of CO_2 in the electrolyte causes an acidification of the media, by Equations (5)-(7), as

$$CO_2\ (aq) + H_2O \leftrightarrow H_2CO_3(aq) \quad (5)$$

$$H_2CO_3(aq) \leftrightarrow H^+ + HCO_3{}^- \qquad (pKa = 6.35) \quad (6)$$

$$HCO_3{}^- \leftrightarrow H^+ + CO_3{}^{2-} \qquad (pKa = 10.33) \quad (7)$$

The liquid electrolyte used in this work was thus a solution of KOH 1M (pH = 14.07), which, after 30 min of bubbling CO_2, was saturated of CO_2 to a pH of 10.5, and this value was kept constant through the electrochemical experimental runs in the CV open vessel. Thus, we expect a mixture of $HCO_3^-/CO_3^{2-}/OH^-$ in the electrolytic solution, which may lead to the formation of methanol, as discussed below.

Keeping in mind that the GDE and MCEs studied in this work were activated in NaOH 1M prior to the CO_2RR experiments, some of the bicarbonate ions generated are expected to be experiencing an ion exchange process as observed in literature [47],

$$CS^+OH^- + HCO_3{}^- \leftrightarrow CS^+HCO_3{}^- + OH^- \quad (8)$$

These were the reactions taking place before the CO_2RR experiments. During the electroreduction process, not only CO_2RR occured, but also HER, which competed with the desired former reaction. For nearly neutral pH conditions usually reported in literature (Table 2), the typical half-reactions at the cathode for the production of methanol were proposed as follows

$$2H^+ + 2e^- \rightarrow H_2 \qquad (E^0 = 0.0V) \qquad (9)$$

$$CO_2 + 6H^+ + 6e^- \rightarrow CH_3OH + H_2O \qquad (E^0 = -0.38V)\ [47,65,66] \qquad (10)$$

However, at high pH values in alkaline electrochemical cells as those used in this work, the reaction mechanism that may be taking place at the cathode is that of hydrogen produced from water electrolysis,[67] (for water electrolysis that was competing with CO_2 electrolysis)

$$H_2O + 2e^- \rightarrow H_2 + OH^- \qquad (E^0 = -0.83V) \qquad (11)$$

Still the information reported in literature about the methanol production mechanism in highly alkaline media is scarce. CO was reported to be an intermediate from CO_2 in most of the possible products, including methanol, and the reaction generally proposed was [4,23]

$$3CO_2 + H_2O + 2e^- \rightarrow CO + 2HCO_3^- \qquad (12)$$

When Cu was used as catalyst in the cathode at pH > 8 in the electrolyte solution, as

$$Cu + 2OH^- \rightarrow Cu(OH)_2^{2-}(Membrane) + 2e^- \qquad (13)$$

$$HCO_3^- + 2e^- \rightarrow CH_2(OH)_2 \qquad (14)$$

The latter species produced in Equations (13)-(14) are unstable and may end up forming CH_3OH [68]. In the production of methanol, 6 electrons are involved in the reaction. Thus, assuming that CO_2RR in alkaline media generates bicarbonate anions as Equation (12) suggested, the half-reaction at the cathode would result in

$$7CO_2 + 5H_2O + 6e^- \rightarrow CH_3OH + 6HCO_3^- \qquad (13)$$

Peterson et al. utilized a Computational Hydrogen Model to obtain the pathways of CO_2RR to HCOOH, CO, CH_4 and CH_3OH on a Cu catalyst.[8] For CH_3OH, CO was generated as intermediate after a two pairs of $e^- + H^+$ transferred to the adsorbed CO_2, liberating a water molecule. Then, an aldehyde was generated after another pair $e^- + H^+$ transferred. The final pair of $e^- + H^+$ promoted methanol formation in water-swollen systems.[11] Periasamy et al. proposed a similar route for MeOH production [47], by

$$CO_2 + 2H^+ + 2e^- \rightarrow CO + H_2O \quad (14)$$

$$CO + 2H^+ + 2e^- \rightarrow H_2CO \quad (15)$$

$$H_2CO + 2H^+ + 2e^- \rightarrow CH_3OH \quad (16)$$

Assuming the participation of the same intermediates in the CO_2RR to methanol in a high alkaline media as that employed in this work, the former equations can be replaced by

$$CO_2 + H_2O + 2e^- \rightarrow CO + 2OH^- \quad (17)$$

$$CO + 2H_2O + 2e^- \rightarrow H_2CO + 2OH^- \quad (18)$$

$$H_2CO + 2H_2O + 2e^- \rightarrow CH_3OH + 2OH^- \quad (19)$$

Leading to the overall half-reaction,

$$CO_2 + 5H_2O + 6e^- \rightarrow CH_3OH + 6OH^- \quad (20)$$

At the anode, the OER takes place, and the half-reaction in high alkaline media would be

$$4OH^- \rightarrow 4e^- + O_2 + 2H_2O \quad (21)$$

Therefore, the OH- generated according to Equation (20), compensated the OH^- consumed in Equation (21), thus explaining the constant pH of 10.5 observed throughout the experimental runs in the present work.

CONCLUSIONS

The design of new membrane coated electrodes (MCEs) prepared from renewable and low-cost polymers, with Cu catalyst embedded in different forms in the membrane over-layer and as Cu nanoparticles (NPs) in the catalytic layer, where chitosan biopolymer (CS) was also used as binder, by a simple and effective method to ensure the intimate connection between the ionic biopolymer and the catalyst, as well as enhanced electrode stability in the CO_2 electroreduction towards methanol was studied. The behavior of the MCEs was analyzed in high alkaline media and compared with that of Cu plate and an uncoated gas diffusion (GDE) electrode without membrane over-layer. The membrane over-layer was an alkaline anion exchange membrane (AAEM) with previously tuned hydrophilicity, ion-exchange capacity, anion conductivity, mechanical and permeability properties, based on the mixed matrix membrane (MMM) approach by the addition of inorganic fillers: Cu NPs, Cu-exchanged layered stannosilicate UZAR-S3 and Cu-exchanged zeolite Y in the CS:PVA polymer matrix. The behavior of the MCE enhanced the performance of the uncoated GDE, avoiding material losses and Faradaic Efficiency (FE) towards methanol. The MCE performance measured in a three electrode open electrochemical cell showed promising results in terms of FE towards methanol, with a value of 68.05% in the case of the Cu-Y/CS:PVA MCE. It was expected that these renewable or economic polymers were adequate for membrane coating preparation, and the membrane over-layer kept the conditions of humidity and conductivity along the experiment, thus providing protection and higher stability to the catalyst and electrode. When the membrane over-layer was functionalized by the inclusion of ion-exchangeable inorganic fillers, the physicochemical properties and electrode activity were improved, but the membrane over-layer was partially dissolved upon reaction and entered the

pores of the carbonaceous substrate beneath. Further work should be directed to the understanding of the role of the membrane over-layer from the MMM non-idealities,[62] which agreed with those observed in the electrochemical reduction of CO_2 to CH_3OH, as well as investigating the performance in a continuous flow filter press cell reactor where the closed environment is expected to prevent the local effects affecting the overall performance, as well as allowing us to complete the mass balance by measuring the gas phase. This way, current system limitations, *i.e.* no division between the electrodes, which could cause re-oxidation of methanol at the anode or the low solubility of CO_2 in aqueous solutions, could be overcome.

NOMENCLATURE

Abbreviation	**Description**
AAEM	Alkaline anion exchange membrane
CCM	Catalyst Coated Membrane
CEM	Cation exchange membrane
CO_2RR	CO_2 Reduction Reaction
CS	Chitosan biopolymer
FE	Faradaic Efficiency
GDE	Gas Diffusion Electrode
MCE	Membrane coated electrode
MCEC	Membrane coated electrocatalyst
MMM	Mixed Matrix Membrane
NP	Nanoparticle
Ppy	Polypyrrole

PVA	Poly vinyl alcohol
RHE	Reversible Hydrogen Electrode
Symbol	
A	working electrode geometric area, cm^2
b	Membrane over-layer thickness in Equation (3)
C	Dissolved CO_2 concentration in saturated solution, M
D	Diffusion coefficient, cm^2/s, in Equation (29)
δ	Diffusion layer thickness, cm
F	Faraday constant (96484.5 C/mol)
$\mathbf{I_{ss}}$	steady state current in Equation (2)
j	Experimental current density, mA/cm^2
n	Moles of product generated
q	Total charge applied, Coulombs
v	estimated average CO_2 flow rate, cm/s
z	Number of exchanged electrons

AUTHOR CONTRIBUTIONS

The manuscript was written through contributions of all authors.

ACKNOWLEDGMENTS

Financial support from the Spanish Ministry of Science and Universities under project grant CTQ2016-76231-C2-1-R is gratefully acknowledged. A.M.M. also acknowledges the FPI

grant no. BES-2017-080795. Prof. Manuel Arruebo (Instituto de Nanociencia de Aragón, Universidad de Zaragoza) is also gratefully acknowledged for providing the SEM-EDX measurements. Anonymous reviewers are also deeply thanked for their insightful comments.

KEYWORDS

CO_2 electroreduction; membrane coated electrodes; alkaline medium; methanol; chitosan.

REFERENCES

[1] AEMET, "AEMET," **2019**.

[2] NOAA, *Trends Atmos. Carbon Dioxide* **2019**.

[3] E. I. Koytsoumpa, C. Bergins, E. Kakaras, *J. Supercrit. Fluids* **2018**, *132*, 3–16.

[4] W. Yang, K. Dastafkan, C. Jia, C. Zhao, *Adv. Mater. Technol.* **2018**, *3*, 1–20.

[5] G. O. Larrazábal, A. J. Martín, J. Pérez-Ramírez, *J. Phys. Chem. Lett.* **2017**, *8*, 3933–3944.

[6] F. Herrera, H. Gómez, R. Schrebler, P. Cury, R. Córdova, *J. Electroanal. Chem.* **2002**, *516*, 23–30.

[7] B. Endrődi, G. Bencsik, F. Darvas, R. Jones, K. Rajeshwar, C. Janáky, *Prog. Energy Combust. Sci.* **2017**, *62*, 133–154.

[8] A. A. Peterson, F. Abild-Pedersen, F. Studt, J. Rossmeisl, J. K. Nørskov, *Energy Environ. Sci.* **2010**, *3*, 1311–1315.

[9] K. P. Kuhl, E. R. Cave, D. N. Abram, T. F. Jaramillo, *Energy Environ. Sci.* **2012**, *5*, 7050–7059.

[10] S. Nitopi, E. Bertheussen, S. B. Scott, X. Liu, A. K. Engstfeld, S. Horch, B. Seger, I. E. L. Stephens, K. Chan, C. Hahn, et al., *Chem. Rev.* **2019**, *119*, 7610–7672.

[11] S. Xu, E. A. Carter, *Chem. Rev.* **2019**, *119*, 6631–6669.

[12] Y. Song, R. Peng, D. K. Hensley, P. V. Bonnesen, L. Liang, Z. Wu, H. M. Meyer, M. Chi, C. Ma, B. G. Sumpter, et al., *ChemistrySelect* **2016**, *1*, 6055–6061.

[13] P. Huang, S. Ci, G. Wang, J. Jia, J. Xu, Z. Wen, *J. CO2 Util.* **2017**, *20*, 27–33.

[14] M. Peng, S. Ci, P. Shao, P. Cai, Z. Wen, *J. Nanosci. Nanotechnol.* **2019**, *19*, 3232–3236.

[15] J. Albo, M. Perfecto-Irigaray, G. Beobide, A. Irabien, *J. CO2 Util.* **2019**, *33*, 157–165.

[16] H. Deng, D. Wang, R. Wang, X. Xie, Y. Yin, Q. Du, K. Jiao, *Appl. Energy* **2016**, *183*, 1272–1278.

[17] W. Lee, Y. E. Kim, M. H. Youn, S. K. Jeong, K. T. Park, *Angew. Chemie - Int. Ed.* **2018**, *57*, 6883–6887.

[18] P. Kang, S. Zhang, T. J. Meyer, M. Brookhart, *Angew. Chemie - Int. Ed.* **2014**, *53*, 8709–8713.

[19] C. Dinh, T. Burdyny, G. Kibria, A. Seifitokaldani, C. M. Gabardo, F. P. G. de Arquer, A. Kiani, J. P. Edwards, P. De Luna, O. S. Bushuyev, et al., *Science (80-.).* **2018**, *787*, 783–787.

[20] D. M. Weekes, D. A. Salvatore, A. Reyes, A. Huang, C. P. Berlinguette, *Acc. Chem. Res.* **2018**, *51*, 910–918.

[21] J. Ran, L. Wu, Y. He, Z. Yang, Y. Wang, C. Jiang, L. Ge, E. Bakangura, T. Xu, *J. Memb. Sci.* **2017**, *522*, 267–291.

[22] C. Delacourt, P. L. Ridgway, J. B. Kerr, J. Newman, *J. Electrochem. Soc.* **2007**, *155*, B42.

[23] I. Merino-Garcia, E. Alvarez-Guerra, J. Albo, A. Irabien, *Chem. Eng. J.* **2016**, *305*, 104–120.

[24] H. P. Yang, S. Qin, H. Wang, J. X. Lu, *Green Chem.* **2015**, *17*, 5144–5148.

[25] G. Díaz-Sainz, M. Alvarez-Guerra, J. Solla-Gullón, L. García-Cruz, V. Montiel, A. Irabien, *J. CO2 Util.* **2019**, *34*, 12–19.

[26] J. Qiu, J. Tang, J. Shen, C. Wu, M. Qian, Z. He, J. Chen, S. Shuang, *Electrochim. Acta* **2016**, *203*, 99–108.

[27] Z. Yin, H. Peng, X. Wei, H. Zhou, J. Gong, M. Huai, X. Li, G. Wang, J. Lu, L. Zhuang, *Energy Environ. Sci.* **2019**, *10.1039/C9*, 0–19.

[28] R. B. Kutz, Q. Chen, H. Yang, S. D. Sajjad, Z. Liu, I. R. Masel, *Energy Technol.* **2017**, *5*, 929–936.

[29] H. Yang, J. J. Kaczur, S. D. Sajjad, R. I. Masel, *J. CO2 Util.* **2017**, *20*, 208–217.

[30] S. Ma, M. Sadakiyo, R. Luo, M. Heima, M. Yamauchi, P. J. A. Kenis, *J. Power Sources* **2016**, *301*, 219–228.

[31] J. Qi, N. Benipal, H. Wang, D. J. Chadderdon, Y. Jiang, W. Wei, Y. H. Hu, W. Li, *ChemSusChem* **2015**, *8*, 1147–1150.

[32] L. M. Aeshala, R. G. Uppaluri, A. Verma, *J. CO2 Util.* **2013**, *3–4*, 49–55.

[33] S. Ren, D. Joulié, D. Salvatore, K. Torbensen, M. Wang, M. Robert, C. P. Berlinguette, *Science (80-.).* **2019**, *365*, 367–369.

[34] L. García-Cruz, C. Casado-Coterillo, J. Iniesta, V. Montiel, A. Irabien, *J. Appl. Polym. Sci.* **2015**, *132*, 1–10.

[35] J. Ma, Y. Sahai, *Carbohydr. Polym.* **2013**, *92*, 955–975.

[36] Y. Wan, B. Peppley, K. A. M. Creber, V. T. Bui, E. Halliop, *J. Power Sources* **2008**, *185*, 183–187.

[37] L. García-Cruz, C. Casado-Coterillo, J. Iniesta, V. Montiel, A. Irabien, *J. Memb. Sci.* **2016**, *498*, 395–407.

[38] D. V. Esposito, *ACS Catal.* **2018**, *8*, 457–465.

[39] N. Y. Labrador, E. L. Songcuan, C. De Silva, H. Chen, S. J. Kurdziel, R. K. Ramachandran, C. Detavernier, D. V. Esposito, *ACS Catal.* **2018**, *8*, 1767–1778.

[40] Y. Lin, H. Li, C. Liu, W. Xing, X. Ji, *J. Power Sources* **2008**, *185*, 904–908.

[41] T. R. O'Toole, T. J. Meyer, B. Patrick Sullivan, *Chem. Mater.* **1989**, *1*, 574–576.

[42] R. Aydin, H. Ö. Doğan, F. Köleli, *Appl. Catal. B Environ.* **2013**, *140–141*, 478–482.

[43] S. Ponnurangam, C. M. Yun, I. V. Chernyshova, *ChemElectroChem* **2016**, *3*, 74–82.

[44] Y. Hori, H. Ito, K. Okano, K. Nagasu, S. Sato, *Electrochim. Acta* **2003**, *48*, 2651–2657.

[45] M. Berggren, G. G. Malliaras, *Science (80-.).* **2019**, *364*, 233–234.

[46] S. Ponnurangam, C. M. Yun, I. V. Chernyshova, *ChemElectroChem* **2016**, *3*, 74–82.

[47] A. P. Periasamy, R. Ravindranath, S. M. Senthil Kumar, W. P. Wu, T. R. Jian, H. T. Chang, *Nanoscale* **2018**, *10*, 11869–11880.

[48] A. Marcos-Madrazo, C. Casado-Coterillo, L. García-Cruz, J. Iniesta, L. Simonelli, V. Sebastián, M. Encabo-Berzosa, M. Arruebo, A. Irabien, *Polymers (Basel).* **2018**, *10*, 913.

[49] K. P. Kuhl, E. R. Cave, D. N. Abram, T. F. Jaramillo, *Energy Environ. Sci.* **2012**, *5*, 7050–7059.

[50] A. J. Varma, S. V Deshpande, J. F. Kennedy, *Carbohydr. Polym.* **2004**, *55*, 77–93.

[51] J. Li, K. Chang, H. Zhang, M. He, W. A. Goddard, J. G. Chen, M. J. Cheng, Q. Lu, *ACS Catal.* **2019**, *9*, 4709–4718.

[52] W. Lv, J. Bei, R. Zhang, W. Wang, F. Kong, L. Wang, W. Wang, *ACS Omega* **2017**, *2*, 2561–2567.

[53] D. Sebastián, A. Palella, V. Baglio, L. Spadaro, S. Siracusano, P. Negro, F. Niccoli, A. S. Aricò, *Electrochim. Acta* **2017**, *241*, 28–40.

[54] J. Yuan, M. P. Yang, Q. L. Hu, S. M. Li, H. Wang, J. X. Lu, *J. CO2 Util.* **2018**, *24*, 334–340.

[55] B. C. Marepally, C. Ampelli, C. Genovese, F. Tavella, L. Veyre, E. A. Quadrelli, S. Perathoner, G. Centi, *J. CO2 Util.* **2017**, *21*, 534–542.

[56] J. Albo, A. Sáez, J. Solla-Gullón, V. Montiel, A. Irabien, *Appl. Catal. B Environ.* **2015**, *176–177*, 709–717.

[57] A. N. Grace, S. Y. Choi, M. Vinoba, M. Bhagiyalakshmi, D. H. Chu, Y. Yoon, S. C. Nam, S. K. Jeong, *Appl. Energy* **2014**, *120*, 85–94.

[58] S. Ahn, R. J. Wakeham, J. A. Rudd, A. R. Lewis, S. Alexander, E. Andreoli, K. Klyukin, V. Alexandrov, F. Carla, *ACS Catal.* **2018**, *8*, 4132–4142.

[59] J. T. Billy, A. C. Co, *ACS Catal.* **2017**, *7*, 8467–8479.

[60] N. Gupta, M. Gattrell, B. MacDougall, *J. Appl. Electrochem.* **2006**, *36*, 161–172.

[61] H. Zhang, R. Guo, J. Zhang, X. Li, *ACS Appl. Mater. Interfaces* **2018**, *10*, 43031–43039.

[62] C. Casado-Coterillo, A. Fernández-Barquín, S. Valencia, A. Irabien, *Membranes (Basel).* **2018**, *8*, DOI 10.3390/membranes8020032.

[63] Y. Hori, in *Mod. Asp. Electrochem.* (Eds.: C.G. Vayenas, R.E. White), Springer, New York, **2008**, pp. 89–189.

[64] O. G. Sánchez, Y. Y. Birdja, M. Bulut, J. Vaes, T. Breugelmans, D. Pant, *Curr. Opin. Green Sustain. Chem.* **2019**, *16*, 47–56.

[65] W. Yang, K. Dastafkan, C. Jia, C. Zhao, *Adv. Mater. Technol.* **2018**, *3*, 1–20.

[66] E. S. C. Tsang, Lin Ye, Weiran Zheng, H. W. Man, *Energy Technol.* **2018**, 119–190.

[67] C. Graves, S. D. Ebbesen, M. Mogensen, K. S. Lackner, *Renew. Sustain. Energy Rev.* **2011**, *15*, 1–23.

[68] A. Palacios-Padrós, F. Caballero-Briones, I. Díez-Pérez, F. Sanz, *Electrochim. Acta* **2013**, *111*, 837–845.

Table of Contents

Membrane-coated electrodes have been prepared by coating the electrode with a mixed matrix layer of chitosan and polyvinyl alcohol with non-toxic inorganic fillers; their performance in CO_2 electroreduction to methanol in alkaline media has been evaluated.